Journal of Mathematics and Modeling in Finance (JMMF)
Vol. 7, No. 1, Winter & Spring 2027
Research paper

Clustered Cryptocurrency Risk Momentum and Portfolio Performance : Identifying Homogeneous Risk Groups

Mohaddeseh Yaghtin[1], **Abbas Saghaei**[2], **Seyed Ahmad Yazdian**[3], **Majid Mirzaee Ghazani**[4]

[1] Department of Industrial Engineering, SR.C., Islamic Azad University, Tehran, Iran.
m.yaghtin@iau.ac.ir

[2] Department of Industrial Engineering, SR.C., Islamic Azad University, Tehran, Iran.
a.saghaei@iau.ac.ir

[3] Department of Industrial Engineering, SR.C., Islamic Azad University, Tehran, Iran.
a.yazdian@iau.ac.ir

[4] Department of Industrial Engineering, K. N. Toosi University of Technology, Tehran, Iran.
majidmirzaee@kntu.ac.ir

Abstract:
This paper empirically investigates the performance of a factor-based "risk momentum" strategy within the cryptocurrency market, utilizing a K-Means clustering approach to identify homogeneous risk groups. We apply a multi-stage methodology to hourly cryptocurrency data, encompassing variable extraction, cross-sectional regressions to derive risk components, and K-Means clustering to group assets based on their historical risk profiles. Market-capitalization-weighted long-short portfolios are constructed by aggregating cryptocurrencies from the lowest and highest risk deciles across all identified clusters. Empirical analysis reveals that the overall clustered risk momentum strategy yielded statistically significant negative returns during the study period. This suggests a "risk reversal" phenomenon in the aggregated portfolio rather than positive risk momentum. Furthermore, we provide a theoretical explanation for this phenomenon using a stochastic Ornstein-Uhlenbeck mean-reversion model, mathematically demonstrating how the speed of price correction outweighs momentum persistence in high-frequency cryptocurrency data.

Keywords: Cryptocurrency, Risk momentum, K-Means clustering, Portfolio strategy, Intraday trading, Market anomalies.
Classification: 91G15; 62H30; 60H10.

1 Introduction

The global financial landscape has been significantly reshaped by the emergence of the cryptocurrency market. Its distinct characteristics, including 24/7 trading, decentralization, and high volatility, present both novel opportunities and considerable challenges for conventional asset pricing theories [2, 3]. While market anomalies such as momentum are well-documented in traditional equity markets [8], their applicability in the digital asset space requires dedicated empirical validation [22]. The growing complexity of this market necessitates the use of more sophisticated

[2]Corresponding author
Received: 14/04/2026 Accepted: 26/06/2026
10.22054/jmmf.2026.92203.1277

analytical tools to uncover underlying patterns [19].

A recent and promising advancement in this domain is the concept of "risk momentum," which posits that the component of asset returns attributable to common risk factors exhibits strong persistence [10]. This framework suggests that sorting assets based on their past risk profiles, rather than raw returns, can yield robust and profitable strategies. However, given the distinct high-volatility nature of digital assets, we explicitly investigate the competing hypothesis that mean-reversion dynamics may dominate momentum effects at high-frequency intervals, potentially leading to risk reversal rather than continuation.

While the body of literature on cryptocurrency portfolio management is growing [13, 18, 25], the intersection of risk momentum and the market's inherent structural heterogeneity remains largely unexplored. The cryptocurrency market is not a monolith; it comprises thousands of assets with diverse risk-return characteristics. A critical challenge lies in structuring this complexity. This paper addresses this challenge by adopting a data-driven clustering approach. We employ the K-Means algorithm to group cryptocurrencies into homogeneous clusters based on their historical risk profiles, thereby identifying natural, data-informed market segments.

Despite the growing interest in risk-based strategies, a significant gap remains in understanding how high-frequency dynamics interact with cross-sectional risk factors within the highly segmented cryptocurrency market. This study is primarily motivated by the need to bridge this gap; we explicitly investigate whether the risk momentum anomaly persists or if it succumbs to the rapid mean-reversion characteristics inherent in digital assets. Therefore, the primary objective of this research is to evaluate the performance of an aggregated risk momentum strategy constructed from dynamically identified clusters. Specifically, we form a market-capitalization-weighted long-short portfolio by taking a long position in the lowest-risk assets and a short position in the highest-risk assets, aggregated across all clusters. This allows us to test the overall efficacy of the risk momentum anomaly when applied to a market structured by its own internal risk dynamics. Ultimately, our work contributes by providing a novel, data-driven perspective on risk-based strategy performance and offers valuable insights into the complex structure of the cryptocurrency market.

2 Literature Review

The theoretical foundation of this study lies at the confluence of three key areas: market anomalies, the emerging field of cryptocurrency asset pricing, and data-driven market segmentation. The Efficient Market Hypothesis (EMH), which suggests that prices reflect all available information [6], has been consistently challenged by the discovery of market anomalies. The momentum effect, where past performance predicts future returns, remains one of the most robust of these anomalies [8], and its presence has also been documented in cryptocurrency markets [1], though it is not without its limitations, such as periodic crashes [5].

To address these limitations, [10] introduced the "risk momentum" framework. Their research demonstrates that the persistence in returns is primarily driven by the "risk component"—the portion of returns explained by common factors. Sorting on this component yields more stable and pervasive profits. Our study directly applies this theoretical lens to the high-frequency environment of the cryptocurrency market.

The cryptocurrency market itself presents a unique laboratory for testing asset pricing theories. Its 24/7 nature and high volatility distinguish it from traditional markets [4, 9]. While some studies find evidence of inefficiencies [22], others work to identify common risk factors similar to those in equity markets [12]. Other research identifies unique factors influencing cryptocurrency prices, such as market sentiment and network-related metrics [21]. This highlights the need for robust methodologies that can account for the market's unique structure.

Structuring this market is a critical challenge. One approach is manual categorization based on function [24]. An alternative, which this paper adopts, is a data-driven approach using clustering algorithms. K-Means clustering has been successfully applied in finance to group assets based on behavioral similarities, aiding in portfolio construction and risk management [14]. By applying K-Means to the risk profiles of cryptocurrencies, we aim to uncover natural market segments and test the risk momentum hypothesis within this data-driven structure.

3 Theoretical Framework: Stochastic Modeling of Price Dynamics

To provide a rigorous mathematical foundation for our empirical analysis, particularly for the observed risk reversal phenomenon, we model the cryptocurrency market dynamics using a complete probability space (Ω, F, P), where Ω represents the sample space of price paths, F is the sigma-algebra of events, and P is the probability measure. The information flow is captured by the filtration $\{F_t\}_{t\geq 0}$.

3.1 Jump-Diffusion Price Process

Given the distinct characteristics of cryptocurrencies, such as extreme volatility and discontinuous price jumps, a standard Geometric Brownian Motion (GBM) is insufficient. Following [16], we model the price dynamics of asset i, denoted as $P_i(t)$, using a Jump-Diffusion process. The Stochastic Differential Equation (SDE) governing the price is defined as:

$$\frac{dP_i(t)}{P_i(t)} = \mu_i(t)dt + \sigma_i(t)dW_i(t) + d\Big(\sum_{j=1}^{N(t)} V_{i,j}\Big) \tag{1}$$

Where:

(i) $\mu_i(t)$ represents the instantaneous expected return (drift).

(ii) $\sigma_i(t)dW_i(t)$ is the continuous diffusion component, where $W_i(t)$ is a standard Brownian motion modeling normal volatility.

(iii) $N(t)$ is a Poisson process with intensity λ, capturing the frequency of sudden market shocks (jumps).

(iv) $V_{i,j}$, is a non-negative random variable representing the absolute price change induced by the j-th jump.

Applying Itô's Lemma for jump-diffusion processes, the logarithmic return dynamics can be derived. This framework allows us to separate the continuous "risk component" from idiosyncratic jumps, which justifies our factor-based extraction method in the empirical section.

3.2 Mean Reversion in Returns (Ornstein-Uhlenbeck Process)

While prices may exhibit jumps, the profitability of a momentum or reversal strategy depends on the time-series behavior of returns. To theoretically analyze the "Risk Reversal" hypothesis, we assume that the instantaneous logarithmic returns, rt, follow an Ornstein-Uhlenbeck (OU) process [23]. This process explicitly models the tendency of returns to revert to a long-term mean, a key characteristic in high-volatility markets:

$$dr_t = \kappa(\theta - r_t)dt + \sigma dW_t \tag{2}$$

Where:

(i) $\kappa > 0$ is the mean-reversion speed, indicating how quickly returns correct towards the mean.

(ii) θ is the long-term equilibrium mean of the returns.

(iii) σ is the volatility of the return process.

The explicit solution to this SDE for a time step Δt , derived using Itô's formula on the function $f(r,t) = r_t e^{\kappa t}$, is:

$$r_{t+\Delta t} = r_t e^{-\kappa \Delta t} + \theta(1 - e^{-\kappa \Delta t}) + \sigma \int_t^{t+\Delta t} e^{-\kappa(t+\Delta t - s)} dW_s \tag{3}$$

This stochastic formulation provides the necessary mathematical structure to test whether the market is driven by momentum (persistence) or reversal (mean reversion).

4 Methodology

Our methodology is a multi-stage process designed to empirically test the factor-based risk momentum hypothesis within a market structured by K-Means clustering.

4.1 Data and Variable Extraction

Hourly OHLCV data were collected from the Binance exchange, spanning from January 1, 2022, to May 31, 2025. To ensure robustness, we constructed a dynamic universe of the top liquid cryptocurrencies, averaging 115 assets per hour, filtered based on market capitalization and trading volume at each rebalancing point. From this raw data, a set of 14 daily financial and statistical factors were extracted for each asset. These factors include core metrics such as realized volatility, skewness, kurtosis, trading volume, and past returns across multiple time horizons, designed to capture diverse dimensions of asset risk and behavior.

4.2 Return Calculation

To ensure robust statistical properties—specifically the time-additivity and distributional symmetry essential for analyzing high-volatility assets—all empirical analyses employ continuously compounded (logarithmic) returns [11]. For each asset, the return at time t is defined as:

$$r_t = ln(\frac{P_t}{P_{t-1}}) \tag{4}$$

where P_t and P_{t-1} denote the closing prices at times t and $t-1$, respectively.

4.3 Factor Normalization and Risk Component

The extracted daily factors were first normalized using a cross-sectional ranking approach. Subsequently, for each hour, a cross-sectional OLS regression was performed to estimate the relationship between hourly log returns and the normalized factors. The fitted portion of this regression for each asset constitutes its "risk component" ($RISK_{s,d,i}$), which served as the primary sorting variable.

For each hour i of day d, the hourly log return of cryptocurrency s at time d, i ($RET_{s,d,i}$) was regressed against its normalized factor values at time $d-1, j$ ($C_{s,d-1,j}$):

$$RET_{s,d,i} = \alpha_{d,i} + \sum_{j=1}^{p} C_{s,d-1,j}\theta_{d,i,j} + \epsilon_{s,d,i} \tag{5}$$

The "risk component" for each cryptocurrency at each hour was calculated as the dot product of its normalized factor values and the corresponding hourly theta vector derived from the cross-sectional regressions:

$$\widehat{RISK}_{s,d,i} = \sum_{j=1}^{p} C_{s,d-1,j}\widehat{\theta}_{d,i,j} \tag{6}$$

4.4 K-Means Clustering

A key innovation of this study is the application of the **K-Means clustering algorithm** to group cryptocurrencies based on the similarity of their historical risk profiles.

Justification for $\mathbf{K-Means}$: The choice of K-Means was driven by both its established effectiveness and its computational efficiency. Given the high-frequency nature and large volume of our data, more complex hierarchical or density-based clustering algorithms proved to be computationally prohibitive and impractical for implementation. K-Means offers a robust and scalable solution for partitioning the dataset into a predefined number of clusters (k=10 in this study), making it a pragmatic choice for large-scale financial analysis [15]. This parameter k=10 was selected based on preliminary stability tests to ensure sufficient granularity for capturing distinct risk profiles while maintaining interpretability and adequate cluster sizes. The algorithm aims to minimize the within-cluster sum of squares (WCSS), which is the objective function:

$$WCSS = \sum_{i=1}^{k} \sum_{x \in C_i} \left|\left|x - \mu_i\right|\right|^2 \tag{7}$$

Where k is the number of clusters (10 in this study), C_i is the i-th cluster, x is a data point (an asset's historical risk profile) in cluster C_i, and μ_i is the centroid (mean) of cluster C_i [7]. Before clustering, the time-series of risk data for each asset was scaled to ensure that all assets contribute equally to the distance calculations. The algorithm then partitioned the assets into 10 distinct clusters, where each cluster contains cryptocurrencies with the most similar historical risk dynamics.

4.5 Decile Ranking and Portfolio Construction

Following the clustering, for each hour, assets were sorted based on their current risk component within each of the 10 clusters. They were then assigned to deciles (1 to 10). The central strategy of this paper, the "Overall Clustered Risk" portfolio, was then constructed. This is a market-capitalization-weighted long-short portfolio formed by aggregating assets from the extreme deciles across all clusters.The weight (w_i) of each asset i in the long and short legs of the portfolio was determined by its market capitalization ($MCap_i$) relative to the total market capitalization of its respective leg (Long or Short):

$$w_i = \frac{MCap_i}{\sum_{j \in Leg} MCap_j} \tag{8}$$

The portfolio aggregated these positions:

(i) **Long Position** : Market-cap-weighted portfolio of assets in Decile 1 (lowest risk) from all 10 clusters.

(ii) **Short Position** : Market-cap-weighted portfolio of assets in Decile 10 (highest risk) from all 10 clusters.

The final long-short portfolio return (R_p) at time t is the difference between the returns of the long (R_L) and short (R_S) legs:

$$R_{p,t} = R_{L,t} - R_{S,t} \tag{9}$$

4.6 Performance Evaluation

The portfolio's performance was evaluated using standard financial metrics, including the Annualized Sharpe Ratio [20] and t-statistics. The Annualized Sharpe Ratio was calculated as:

$$Sharpe\ Ratio = \frac{E[R_p - R_f]}{\sigma_p} \times \sqrt{N} \tag{10}$$

Where $E[R_p - R_f]$ is the expected excess return of the portfolio over the risk-free rate (assumed to be zero), σ_p is the standard deviation of the portfolios excess returns, and N is the number of periods per year (e.g., 365×24 for hourly data). All reported t-statistics were computed using Newey-West heteroskedasticity and autocorrelation consistent (HAC) standard errors [17] to ensure robust statistical inference. The t-statistic for the mean return ($\overline{R}$) was calculated as:

$$t - stat = \frac{\overline{R}}{SE_{HAC}(\overline{R})} \tag{11}$$

Where $SE_{HAC}(\overline{R})$ is the Newey-West standard error of the mean return.

4.7 Numerical Implementation Details

All numerical implementations, including data preprocessing, K-Means clustering, and portfolio backtesting, were executed using Python (version 3.10) with standard scientific computing libraries (e.g., pandas, numpy, and scikit-learn). The K-Means algorithm was initialized using the 'k-means++' method with a maximum of 300 iterations and a tolerance of $1e - 4$ to ensure strict convergence. For the heatmap visualizations (Figures 2 and 3), the signal formation periods (M) and holding periods (N) were parameterized across a comprehensive grid ranging from 1 to 120 hours. This grid was specifically designed to robustly capture both ultra-short-term microstructure effects and multi-day market dynamics.

For the core baseline strategy presented in the main empirical results (Tables 1 -2, Figures 1,4), the specific numerical parameters applied are uniformly set to: $k = 10$ clusters, signal formation period $M = 1$ hour, and holding period $N = 1$ hour. Portfolios are constructed using the extreme risk deciles (Long Decile 1, Short Decile 10) drawn from a dynamic universe of approximately 115 liquid assets. The strategy enforces dynamic hourly rebalancing utilizing market-capitalization weights, and all reported values represent gross logarithmic returns to isolate the core anomaly prior to transaction costs.

5 Empirical Results

This section presents the empirical performance of the "Overall Clustered Risk (KMeans)" long-short portfolio, utilizing log returns.

5.1 Portfolio Performance

The empirical performance of the "Overall Clustered Risk" long-short portfolio reveals significant and pervasive patterns within the high-frequency cryptocurrency market. Table 1 displays the hourly mean returns and robust t-statistics for the strategy. As observed, the portfolio exhibits consistently negative mean returns across all hours of the day. The average return across all hours is -0.92%, which is highly statistically significant with a t-statistic of -115.65.

Table 1: Hourly Performance of the Overall Clustered Risk Portfolio.

Hour	00:00	01:00	02:00	03:00	04:00	05:00	06:00	07:00	08:00	09:00	10:00	11:00
Return (%)	-1.15	-1.03	-0.93	-0.82	-0.92	-0.88	-0.90	-0.92	-0.91	-0.81	-0.82	-0.80
T.stat	(-25.06)	(-28.50)	(-25.26)	(-28.19)	(-22.28)	(-25.96)	(-30.14)	(-25.18)	(-28.56)	(-28.04)	(-26.30)	(-28.23)

Hour	12:00	13:00	14:00	15:00	16:00	17:00	18:00	19:00	20:00	21:00	22:00	23:00	All
Return (%)	-0.97	-0.98	-1.03	-1.08	-1.02	-0.93	-0.84	-0.85	-0.85	-0.82	-0.89	-0.82	-0.92
T.stat	(-25.59)	(-28.26)	(-26.42)	(-25.15)	(-27.32)	(-27.67)	(-27.53)	(-26.92)	(-22.66)	(-24.73)	(-16.85)	(-21.71)	(-115.65)

In Table 1, the hourly performance breakdown explicitly demonstrates the immediate intraday effect of the baseline parameters ($k = 10$ clusters, $M = 1$,$N = 1$). For instance, the highly significant overall average hourly return of -0.92% ($t - stat = -115.65$) mathematically validates that taking a market-capitalization-weighted long position in the lowest risk decile (Decile 1) and a short position in the highest risk decile (Decile 10) yields pervasive underperformance consistently across all 24 individual hours.

This initial robust finding strongly indicates the presence of a "risk reversal" phenomenon, where low-risk assets systematically underperformed high-risk assets on an hourly basis. The economic magnitude of this reversal suggests a powerful market dynamic rather than a mere statistical anomaly. Furthermore, this negative performance persists across various intraday holding periods. Table 2 presents the intraday annualized returns, which remain overwhelmingly negative and statistically significant. The annualized returns (R_{ann}) are calculated from mean hourly returns

$(\overline{R_{hourly}})$ using the total number of hours in a year ($N = 8760$):

$$R_{ann} = \overline{R_{hourly}} \times N \tag{12}$$

Table 2: Intraday Annualized Returns of the Overall Clustered Risk Portfolio.

Hour	00:59	01:59	02:59	03:59	04:59	05:59	06:59	07:59	08:59	09:59	10:59	11:59	12:59	13:59	14:59	15:59	16:59	17:59	18:59	19:59	20:59	21:59	22:59	23:59
00:00	-421.11	-795.29	-1134.18	-1432.00	-1767.93	-2089.85	-2417.77	-2754.43	-3086.32	-3382.60	-3681.00	-3972.12	-4324.10	-4680.22	-5055.84	-5449.28	-5821.92	-6161.45	-6466.78	-6776.96	-7088.52	-7388.67	-7711.64	-8011.77
	(-25.061)	(-32.63)	(-34.73)	(-36.46)	(-37.09)	(-38.45)	(-40.10)	(-41.23)	(-42.15)	(-43.18)	(-44.00)	(-44.30)	(-44.61)	(-45.53)	(-45.87)	(-45.83)	(-46.10)	(-46.50)	(-46.95)	(-47.24)	(-47.48)	(-47.27)	(-46.64)	(-45.94)
01:00		-375.18	-713.07	-1010.89	-1346.82	-1668.74	-1996.66	-2333.31	-2665.20	-2961.49	-3259.88	-3551.01	-3902.98	-4259.11	-4634.72	-5028.16	-5400.81	-5740.34	-6045.67	-6355.85	-6667.41	-6967.55	-7290.53	-7590.66
		(-28.50)	(-32.65)	(-35.10)	(-35.94)	(-37.29)	(-39.28)	(-40.5)	(-41.54)	(-42.69)	(-43.49)	(-43.85)	(-44.20)	(-45.10)	(-45.42)	(-45.43)	(-45.81)	(-46.30)	(-46.79)	(-47.12)	(-47.34)	(-47.13)	(-46.42)	(-45.71)
02:00			-337.89	-635.71	-971.64	-1293.56	-1621.48	-1958.13	-2290.02	-2586.31	-2884.70	-3175.83	-3527.80	-3883.93	-4259.54	-4652.99	-5025.63	-5365.16	-5670.49	-5980.67	-6292.23	-6592.38	-6915.35	-7215.48
			(-25.26)	(-30.891)	(-32.61)	(-34.98)	(-37.55)	(-38.99)	(-40.44)	(-41.76)	(-42.73)	(-43.15)	(-43.57)	(-44.63)	(-45.00)	(-45.00)	(-45.42)	(-45.92)	(-46.47)	(-46.80)	(-47.03)	(-46.80)	(-46.06)	(-45.33)
03:00				-297.82	-633.75	-955.67	-1283.59	-1620.24	-1952.13	-2248.42	-2546.81	-2837.94	-3189.91	-3546.04	-3921.65	-4315.10	-4687.74	-5027.27	-5332.60	-5642.78	-5954.34	-6254.48	-6577.46	-6877.59
				(-28.19)	(-29.94)	(-33.43)	(-36.63)	(-38.12)	(-39.87)	(-41.34)	(-42.28)	(-42.78)	(-43.30)	(-44.49)	(-44.84)	(-44.84)	(-45.30)	(-45.82)	(-46.41)	(-46.75)	(-47.01)	(-46.78)	(-45.99)	(-45.22)
04:00					-335.93	-657.85	-985.76	-1322.42	-1654.31	-1950.6	-2248.99	-2540.12	-2892.09	-3248.22	-3623.83	-4017.27	-4389.92	-4729.45	-5034.78	-5344.96	-5656.52	-5956.66	-6279.64	-6579.77
					(-22.28)	(-29.13)	(-33.92)	(-35.78)	(-38.16)	(-39.90)	(-40.98)	(-41.63)	(-42.36)	(-43.77)	(-44.24)	(-44.29)	(-44.80)	(-45.37)	(-45.99)	(-46.35)	(-46.62)	(-46.38)	(-45.61)	(-44.82)
05:00						-321.92	-649.84	-986.50	-1318.39	-1614.67	-1913.07	-2204.19	-2556.17	-2912.29	-3287.91	-3681.35	-4053.99	-4393.52	-4698.85	-5009.03	-5320.59	-5620.74	-5943.71	-6243.84
						(-25.96)	(-33.34)	(-36.34)	(-39.09)	(-40.98)	(-41.83)	(-42.36)	(-43.11)	(-44.47)	(-44.76)	(-44.77)	(-45.22)	(-45.75)	(-46.35)	(-46.76)	(-46.96)	(-46.71)	(-45.76)	(-44.89)
06:00							-327.91	-664.57	-996.46	-1292.75	-1591.14	-1882.27	-2234.24	-2590.37	-2965.98	-3559.42	-3732.07	-4071.60	-4376.93	-4687.11	-4998.67	-5298.81	-5621.79	-5921.92
							(-30.14)	(-33.54)	(-38.08)	(-40.40)	(-41.60)	(-42.17)	(-43.17)	(-44.78)	(-45.00)	(-44.89)	(-45.35)	(-45.83)	(-46.44)	(-46.87)	(-47.05)	(-46.77)	(-45.77)	(-44.85)
07:00								-336.66	-668.55	-964.83	-1263.23	-1554.19	-1906.31	-2262.45	-2638.07	-3031.51	-3404.15	-3743.68	-4049.01	-4359.19	-4670.75	-4970.90	-5293.87	-5594.00
								(-25.18)	(-34.14)	(-37.46)	(-39.27)	(-40.21)	(-41.57)	(-43.39)	(-43.72)	(-43.76)	(-44.38)	(-44.98)	(-45.65)	(-46.15)	(-46.33)	(-46.13)	(-45.09)	(-44.16)
08:00									-332.28	-628.91	-927.66	-1219.12	-1571.51	-1928.05	-2304.10	-2698.01	-3071.09	-3411.02	-3716.70	-4027.25	-4339.17	-4639.67	-4963.02	-5263.50
									(-28.56)	(-34.57)	(-36.83)	(-38.40)	(-39.95)	(-41.80)	(-42.26)	(-42.41)	(-43.17)	(-43.81)	(-44.62)	(-45.26)	(-45.42)	(-45.29)	(-44.17)	(-43.24)
09:00										-296.64	-595.38	-886.84	-1239.23	-1595.77	-1971.83	-2365.73	-2738.81	-3078.74	-3384.42	-3694.97	-4006.89	-4307.39	-4630.74	-4931.22
										(-28.04)	(-33.62)	(-36.72)	(-38.86)	(-41.18)	(-41.73)	(-41.89)	(-42.73)	(-43.42)	(-44.25)	(-44.94)	(-45.09)	(-44.95)	(-43.68)	(-42.74)
10:00											-298.74	-590.21	-942.59	-1299.14	-1675.19	-2069.10	-2442.18	-2782.10	-3087.79	-3398.33	-3710.26	-4010.75	-4334.11	-4634.59
											(-26.30)	(-32.89)	(-36.11)	(-39.35)	(-40.79)	(-40.71)	(-41.66)	(-42.45)	(-43.47)	(-44.18)	(-44.30)	(-44.18)	(-42.84)	(-41.90)
11:00												-291.47	-643.85	-1000.40	-1376.45	-1770.35	-2143.43	-2483.36	-2789.05	-3099.59	-3411.52	-3712.01	-4035.37	-4335.85
												(-28.23)	(-32.52)	(-36.79)	(-38.33)	(-39.07)	(-40.18)	(-41.11)	(-42.25)	(-43.11)	(-43.20)	(-43.19)	(-41.72)	(-40.81)
12:00													-352.39	-708.93	-1084.98	-1478.89	-1851.97	-2191.90	-2497.58	-2808.13	-3120.05	-3420.55	-3743.90	-4044.38
													(-25.57)	(-33.06)	(-35.85)	(-37.26)	(-38.74)	(-39.94)	(-41.26)	(-42.26)	(-42.37)	(-42.44)	(-40.90)	(-40.09)
13:00														-356.96	-732.60	-1126.50	-1499.58	-1839.51	-2145.19	-2455.74	-2767.66	-3068.16	-3391.51	-3692.00
														(-28.26)	(-32.99)	(-35.73)	(-37.75)	(-39.13)	(-40.67)	(-41.75)	(-41.93)	(-42.01)	(-40.38)	(-39.54)
14:00															-376.05	-769.96	-1143.04	-1482.97	-1788.65	-2099.20	-2411.12	-2711.62	-3034.97	-3335.45
															(-26.42)	(-31.69)	(-34.61)	(-36.51)	(-38.42)	(-39.78)	(-40.23)	(-40.43)	(-38.91)	(-38.22)
15:00																-393.90	-766.98	-1106.91	-1412.60	-1723.14	-2035.07	-2335.56	-2658.92	-2959.40
																(-25.15)	(-30.44)	(-33.55)	(-36.32)	(-38.01)	(-38.73)	(-39.06)	(-37.57)	(-36.93)
16:00																	-373.08	-713.01	-1018.69	-1329.24	-1641.16	-1941.66	-2265.01	-2565.49
																	(-27.32)	(-33.13)	(-36.62)	(-38.47)	(-38.87)	(-39.33)	(-36.98)	(-36.19)
17:00																		-339.93	-645.61	-956.16	-1268.08	-1568.58	-1891.93	-2192.41
																		(-27.67)	(-33.13)	(-35.79)	(-36.42)	(-37.51)	(-35.13)	(-34.64)
18:00																			-305.69	-616.23	-928.15	-1228.65	-1552.01	-1852.49
																			(-27.53)	(-33.14)	(-34.37)	(-35.93)	(-33.31)	(-33.07)
19:00																				-310.54	-622.47	-922.97	-1246.32	-1546.80
																				(-26.92)	(-30.32)	(-32.71)	(-30.45)	(-30.64)
20:00																					-311.92	-612.42	-935.78	-1236.26
																					(-22.66)	(-28.67)	(-26.78)	(-27.78)
21:00																						-300.5	-623.85	-924.33
																						(-24.73)	(-24.51)	(-26.05)
22:00																							-323.35	-623.84
																							(-16.85)	(-21.37)
23:00																								-300.48
																								(-21.71)

In Table 2, the annualized figures explicitly translate the intraday gross logarithmic returns into yearly equivalents by scaling them by an assumption of 8,760 trading hours. As a quantitative demonstration of this compounding effect, the core strategy ($k = 10$ clusters, $M = 1$) initiated at hour 00:00 registers an immediate annualized deficit of -421.11% ($t-stat = -25.06$) after just a one-hour holding period. This underperformance deteriorates monotonically as the holding horizon extends, culminating in an extreme annualized loss of -8011.77% ($t - stat = -45.94$) over a full 24-hour intraday cycle. This consistent, severe degradation across all entry hours quantitatively validates the immense economic magnitude of the high-frequency risk reversal anomaly.

This numerical evidence is visually confirmed in Figure 1, which illustrates a steady and significant downward trend in cumulative returns as the holding horizon increases. The pattern holds uniformly across all trading sessions (All Day, Day Session, and Night Session), confirming that the risk reversal effect is a pervasive feature of the aggregated strategy.

In Figure 1, the cumulative return trajectories visualize the failure of the short-term signal ($M = 1$) across extending holding horizons. As an explicit numerical example in Panel (A) "All Day", the baseline strategy (k=10 clusters, Long D1/ Short D10) consistently degrades, reaching a substantial cumulative loss of approximately

-6500 bps at the maximum 120-hour holding limit. This pattern confirms that the reversal effect dominates microstructure dynamics uniformly across all trading sessions.

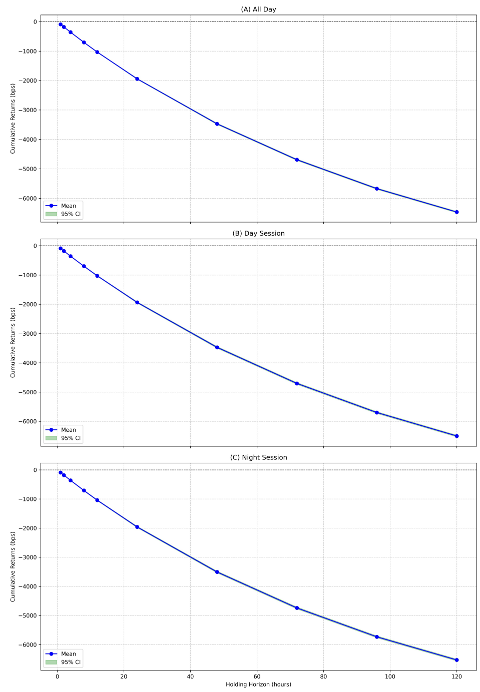

Figure 1: Cumulative Returns (bps) of the Overall Clustered Risk Portfolio across different trading sessions

In Figure 2, the heatmap details the annualized returns across 324 discrete grid combinations of Signal (M) and Holding (N) periods. The severity of the risk reversal is acutely visible in the top-left cell representing the highest frequency implementation ($M = 1, N = 1$), which exhibits an extreme annualized loss of -8019.05%, before progressively moderating at the longest simulated multi-day horizons ($e.g., M = 120, N = 120, yielding - 66.69\%$). Across all cells, portfolios are clustered at k=10 and market-capitalization weighted.

In Figure 3, the Sharpe ratio heatmap systematically confirms the raw return deterioration observed in Figure 2. Evaluated with a zero risk-free rate ($R_f = 0$) and dynamic hourly market-cap weighting, the poorest risk-adjusted performance clearly appears at the shortest intervals, specifically peaking at a severely negative Sharpe ratio of -85.69 in the top-left cell ($M = 1, N = 1$).

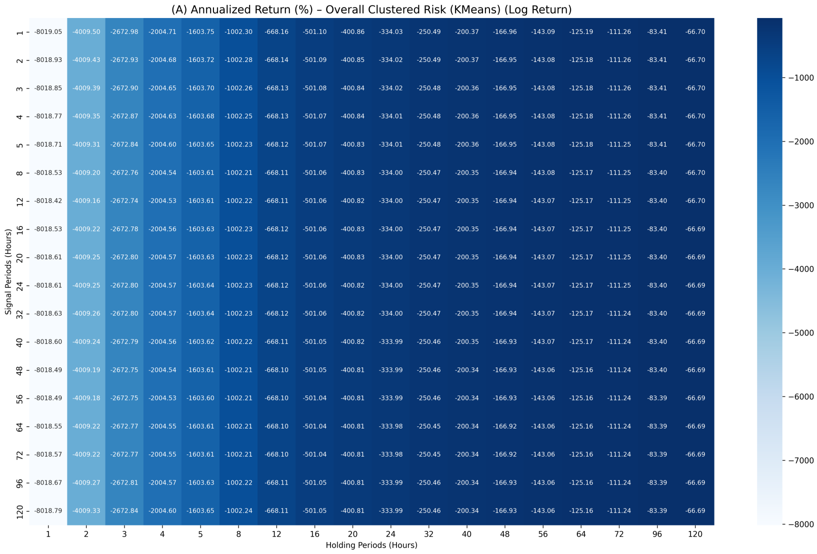

Figure 2: Heatmap of Annualized Returns (%) across a comprehensive parameter grid for Signal (M) and Holding (N) periods.

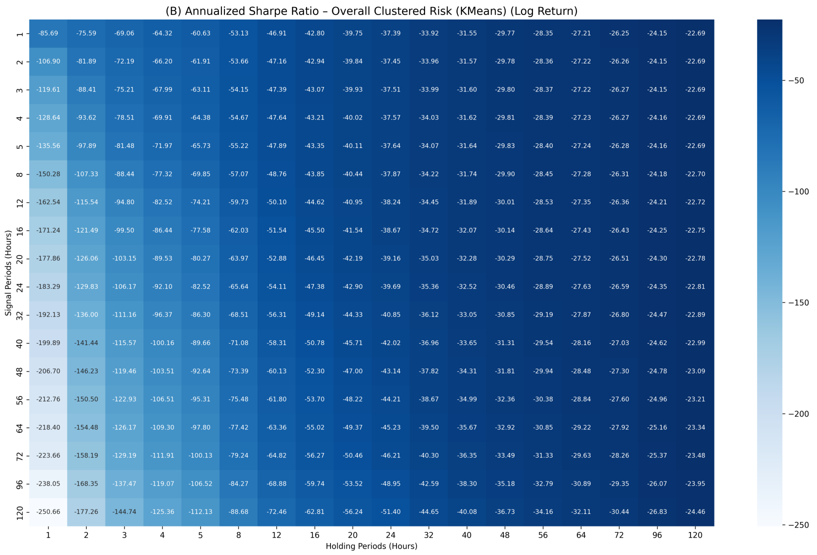

Figure 3: Heatmap of Annualized Sharpe Ratios across varying Signal (M) and Holding (N) periods.

Finally, Figure 4 provides a stark summary of the strategy's overall cumulative performance over the entire sample period on a logarithmic scale. The steep and continuous decline illustrates the severe and compounding losses incurred, confirming that the aggregated long-low-risk, short-high-risk strategy was systematically unprofitable over the long term.

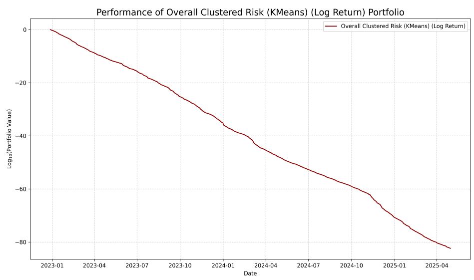

Figure 4: Overall Cumulative Performance of the Clustered Risk Portfolio (Log Scale) from January 2022 to May 2025.

In Figure 4, the overall cumulative performance visualizes the continuous compounding effect of the baseline parameters ($LongD1/ShortD10, M = 1, N = 1$) over the entire 41-month sample. The near-linear downward trajectory on the logarithmic scale, dropping precipitously toward a log-portfolio value of -80 by the end of the period, underscores the robust, long-term persistence of the risk reversal anomaly prior to the deduction of transaction costs.

Given that in high-volatility environments, assets with elevated recent risk exposure tend to exhibit higher concurrent returns (a risk–return relationship), the ranking by risk profile serves as a reasonable proxy for ranking by recent performance. Therefore, we treat the High-Risk leg as the "Winner" leg ($R_{H,t} > \theta$) and the Low-Risk leg as the "Loser" leg ($R_{L,t} < \theta$) in the theoretical analysis that follows.

5.2 Theoretical Explanation of Findings

The empirical results presented in Table 1 and Figure 1 consistently show statistically significant negative returns for the aggregated risk momentum strategy. This implies a "Momentum Failure" and the dominance of a "Risk Reversal" effect. We can now explain this phenomenon mathematically using the Ornstein-Uhlenbeck framework established in Section 3.

Proposition 5.1. *(Momentum Failure under Strong Mean Reversion): If the return process follows an Ornstein-Uhlenbeck dynamics with a high mean-reversion speed κ (as defined in Eq. 3), the expected return of a Long-Short portfolio based on recent past performance will be negative.*

Proof. Consider the conditional expectation of the return at time $t + \Delta t$ given the information at time $t(F_t)$. Due to the martingale property of the Itô integral, the expected value of the stochastic term is zero. Thus:

$$\begin{aligned} E[r_{t+\Delta t}|F_t] =& E[r_t e^{-\kappa \Delta t}|F_t] + E[\theta(1-e^{-\kappa \Delta t})|F_t] \\ &+ E[\sigma \int_t^{t+\Delta t} e^{-\kappa(t+\Delta t - s)} dW_s | F_t] \end{aligned} \tag{13}$$

$$E[r_{t+\Delta t}|F_t] = \theta + (r_t - \theta)e^{-\kappa \Delta t} \tag{14}$$

The expected change in return (expected profit/loss) over the horizon Δt is:

$$E[\Delta r] = E[r_{t+\Delta t} - r_t|F_t] = (\theta - r_t)(1 - e^{-\kappa \Delta t}) \tag{15}$$

For the theoretical analysis that follows, we consider a Long-Short portfolio by buying the "High Risk/Winner" decile (H) where recent returns are high ($r_{H,t} > \theta$) and selling the "Low Risk/Loser" decile (L) where returns are low ($r_{L,t} < \theta$).

(i) **Long Leg (H):** since $r_{H,t} > \theta$, the term $(\theta - r_{H,t})$ is negative. Thus, $E[\Delta r_H] < 0$. The high-risk assets are expected to revert down.

(ii) **Short Leg (L):** since $r_{L,t} < \theta$, the term $(\theta - r_{L,t})$ is positive. Thus, $E[\Delta r_L] > 0$. The low-risk assets are expected to revert up.

The total expected payoff of the portfolio (R_p) is the Long return minus the Short return:

$$E[R_p] = E[\Delta r_H] - E[\Delta r_L] \tag{16}$$

Substituting the expectations:

$$E[R_p] = (\theta - r_{H,t})(1 - e^{-\kappa \Delta t}) - (\theta - r_{L,t})(1 - e^{-\kappa \Delta t}) \tag{17}$$

Simplifying the equation yields:

$$E[R_p] = (r_{L,t} - r_{H,t})(1 - e^{-\kappa \Delta t}) \tag{18}$$

Since by definition of the ranking $r_{H,t} > r_{L,t}$, the term $(r_{L,t} - r_{H,t})$ is strictly negative. Furthermore, since $\kappa > 0$ and $\Delta t > 0$, the term $(1 - e^{-\kappa \Delta t})$ is positive. Therefore,

$$E[R_p] < 0$$

□

This proof demonstrates that in the cryptocurrency market, specifically at the hourly frequency analyzed, the mean reversion parameter κ is sufficiently large that it overpowers any potential momentum persistence. The market efficiently corrects deviations from the mean, causing the "Winners" (High Risk) to underperform and "Losers" (Low Risk) to outperform in the subsequent period, leading to the observed negative profitability of the momentum strategy.

The theoretical model presented here serves primarily as a qualitative framework to explain the mechanism of momentum failure. Detailed calibration of the κ and θ parameters for individual clusters is left for future research.

6 Conclusion and Implications

This study empirically investigated a factor-based "risk momentum" strategy within the cryptocurrency market, employing an innovative K-Means clustering approach. The primary and most striking finding, contrary to the initial hypothesis, was the statistically significant negative performance of the aggregated long-short portfolio. This result unequivocally points to a powerful **"Risk Reversal"** phenomenon during the analyzed period, meaning that high-risk assets systematically outperformed their low-risk counterparts. It is important to note that while this risk reversal phenomenon is statistically robust, its economic exploitability in a real-world high-frequency trading setting would require a further careful assessment of transaction costs and liquidity constraints.

This finding carries significant implications for understanding the structure of the cryptocurrency market. Firstly, it demonstrates that well-known anomalies from traditional financial markets, such as risk momentum, may not be directly or simply generalizable to this new market. The unique dynamics of the crypto space—likely influenced by factors such as retail investor behavior, information asymmetry, and a highly speculative nature—appear to lead to a reward for higher risk-taking. Therefore, investors should approach risk-based strategies that have proven successful in traditional markets with considerable caution.

Secondly, although the aggregated strategy was unprofitable, this research validates the high value of the clustering methodology as an analytical tool for structuring the heterogeneous cryptocurrency market. K-Means clustering provides a robust, data-driven framework for segmenting the market based on inherent similarities in assets' risk profiles. In effect, the failure of the overall strategy shifts the research question from "Does risk momentum exist across the entire market?" to a more nuanced one:

"In which of the identified clusters might risk momentum manifest differently ? "

This framework serves as a cornerstone for future analyses aimed at discovering profitable strategies within specific market segments.

Limitations and Future Research

This study is accompanied by certain limitations that pave the way for future research. The definition of "risk" is contingent on the chosen set of factors, and more dynamic definitions could be developed using more sophisticated models or machine learning techniques. Furthermore, our analysis does not account for transaction costs and liquidity constraints, which are significant in the crypto market. Future research could incorporate models for these costs to provide a more accurate assessment of net strategy profitability. Most importantly, it is recommended that the strategy's performance be analyzed separately **within** each cluster to determine whether the risk reversal phenomenon is uniform across all clusters or if some possess the potential for profitable risk momentum. Examining the strategy's performance across different market regimes (e.g., bull vs. bear markets) could also yield valuable insights.

In conclusion, this research demonstrated that an aggregated factor-based risk momentum strategy was not profitable in the cryptocurrency market during the period studied. However, by uncovering the significant "risk reversal" phenomenon and providing a robust methodological framework, it offers a deeper understanding of the complex interplay between risk and return in this emerging asset class and opens new avenues for future investigation.

Bibliography

[1] H. A. Aalborg, P. Molnár, and J. E. de Vries, *What can explain the price, volatility and trading volume of Bitcoin?*, Finance Research Letters, (2019) 29, 255–265.

[2] D. G. Baur, K. Hong, and A. D. Lee, *Bitcoin: Medium of exchange or speculative assets?*, Journal of Behavioral and Experimental Finance, (2018) 20, 42–55.

[3] P. Ciaian, M. Rajcaniova, and d. A. Kancs, *The economics of BitCoin price formation*, Applied Economics, (2016) 48, No. 19, 1799–1815.

[4] S. Corbet, B. Lucey, and L. Yarovaya, *Datacoin: The new gold? A systematic review of the literature*, International Review of Financial Analysis, (2019) 62, 100–112.

[5] K. Daniel, and T. J. Moskowitz, *Momentum Crashes*, Journal of Financial Economics, (2016) 122, No. 2, 221–247.

[6] E. F. Fama, *Efficient Capital Markets: A Review of Theory and Empirical Work*, The Journal of Finance, (1970) 25, No. 2, 383–417.

[7] T. Hastie, R. Tibshirani, and J. Friedman, *The Elements of Statistical Learning: Data Mining, Inference, and Prediction*, Springer, (2009).

[8] N. Jegadeesh, and S. Titman, *Returns to Buying Winners and Selling Losers: Implications for Stock Market Efficiency*, The Journal of Finance, (1993) 48, No. 1, 65–91.

[9] P. Katsiampa, *Volatility estimation for Bitcoin: A comparison of GARCH models*, Economics Letters, (2017) 158, 3–6.

[10] S. Z. Li, P. Yuan, and G. Zhou, *Risk Momentum: A New Class of Price Patterns*, Working Paper, (2023).

[11] J. Y. Campbell, A. W. Lo, and A. C. MacKinlay, *The Econometrics of Financial Markets*, Princeton University Press, (1997).

[12] Y. Liu, A. Tsyvinski, and X. Wu, *Common Risk Factors in Cryptocurrency*, Journal of Finance, (2022) 77, No. 2, 1133–1178.

[13] Y. Liu, *Portfolio Optimization with Cryptocurrencies*, SSRN Electronic Journal, (2018).

[14] Y. N. Lu, S. P. Li, L. X. Zhong, X. F. Jiang, and F. Ren, *A clustering-based portfolio strategy incorporating momentum effect and market trend prediction*, Chaos, Solitons & Fractals, (2018) 117, 1–15.

[15] J. MacQueen, *Some methods for classification and analysis of multivariate observations*, Proceedings of the Fifth Berkeley Symposium on Mathematical Statistics and Probability, (1967).

[16] R. C. Merton, *Option pricing when underlying stock returns are discontinuous*, Journal of Financial Economics, (1976).

[17] W. K. NEWEY, AND K. D. WEST, *A Simple, Positive Semi-Definite, Heteroskedasticity and Autocorrelation Consistent Covariance Matrix*, ECONOMETRICA, (1987) 55, No. 3, 703–708.

[18] E. PLATANAKIS, C. SUTCLIFFE, AND S. ZIKOVIC, *Cryptocurrency Portfolio Optimization*, JOURNAL OF ALTERNATIVE INVESTMENTS, (2018) 21, No. 3, 69–82.

[19] H. SEBASTIAO, AND P. GODINHO, *Forecasting cryptocurrency returns: A comparison of machine learning models*, EUROPEAN JOURNAL OF FINANCE, (2021) 27, No. 13, 1264–1290.

[20] W. F. SHARPE, *Mutual Fund Performance*, THE JOURNAL OF BUSINESS, (1966) 39, No. 1, 119–138.

[21] Y. SOVBETOV, *Factors influencing cryptocurrency prices: Evidence from Bitcoin, Ethereum, Dash, Litcoin, and Monero*, JOURNAL OF ECONOMICS AND FINANCIAL ANALYSIS, (2018) 2, No. 2, 1–27.

[22] A. URQUHART, *The inefficiency of Bitcoin*, ECONOMICS LETTERS, (2016) 148, 80–82.

[23] O. VASICEK, *An equilibrium characterization of the term structure*, JOURNAL OF FINANCIAL ECONOMICS, (1977).

[24] S. ZIKOVIC, B. TOMIC, AND M. CULJAK, *Benefits of sectoral cryptocurrency portfolio optimization*, RESEARCH IN INTERNATIONAL BUSINESS AND FINANCE, (2021) 59, 101615.

[25] K. FIROUZI, *Stochastic Dynamics of Ripple XRP for Cross-Border Settlement Optimization*, JOURNAL OF MATHEMATICS AND MODELING IN FINANCE (JMMF), (2026) 6, No. 2, 19–41.

How to Cite: Mohaddeseh Yaghtin[1], Abbas Saghaei[2], Seyed Ahmad Yazdian[3], Majid Mirzaee Ghazani[4], *Clustered Cryptocurrency Risk Momentum and Portfolio Performance : Identifying Homogeneous Risk Groups*, Journal of Mathematics and Modeling in Finance (JMMF), Vol. 7, No. 1, Pages:111–126, (2027).